

1 O-atom production in water ice: Implications for O₂ formation on icy 2 satellites

3 Paul D. Cooper¹, Marla H. Moore² and Reggie L. Hudson^{2,3}

5 ¹ Department of Chemistry and Biochemistry

6 George Mason University

7 4400 University Drive

8 Fairfax, VA 22030

9

10 ² NASA/Goddard Space Flight Center

11 Astrochemistry Branch, Code 691

12 Greenbelt, MD 20771, USA

13

14 ³ Department of Chemistry

15 Eckerd College

16 4200 54th Avenue South

17 St. Petersburg, FL 33711, USA

18

19 Number of Manuscript Pages: 18

20 Tables: 2 Figures: 3

21 TOTAL NUMBER OF PAGES: 18

22 **Keywords:** Planets and Satellites: individual (*Ganymede, Europa*); planets; rings

23 astrochemistry, molecular processes

24

25 ABSTRACT

26 We have found that O-atoms are a primary product in the irradiation of water-ice with 0.8
27 MeV protons. This observation has implications in understanding the chemical reactions
28 that occur to produce molecular oxygen (O_2) in such laboratory ices, as well as ices found
29 on the surfaces of Ganymede and Europa, and the ice particles present in Saturn's rings.
30 We estimate that in irradiated water-ice O_2 can be formed at a lower limit of 0.07% by
31 number relative to water and is in agreement with observations of the icy Jovian
32 satellites.

33

34 MAIN TEXT

35 There have been several recent laboratory investigations of the formation of molecular
36 oxygen from irradiated water ice (Orlando and Sieger et al., 2003; Petrik et al., 2005;
37 Teolis et al., 2006). The formation of oxygen is of particular interest in the formation of
38 O_2 on the surface of the icy Galilean satellites (Spencer et al., 1995; Spencer and Calvin,
39 2002) and also an O_2 atmosphere associated with Saturn's rings (Tokar et al., 2005;
40 Johnson et al., 2006). In both cases, O_2 is postulated to be formed from the radiolytic
41 and/or photolytic destruction of H_2O molecules in the ices of these objects.

42

43 Despite ongoing efforts from various research groups, there is still a void in our
44 understanding of the chemical processes that form O_2 molecules in irradiated water ice.
45 The problem is not helped by the weak electronic and vibrational transitions of O_2 that
46 make detecting solid-phase O_2 by optical spectroscopic methods difficult. Consequently,

47 the detection of O₂ is commonly performed by quadrupole mass spectrometry (QMS) of
48 molecules sputtered during the irradiation process, or later released in temperature
49 programmed desorption (TPD) experiments.

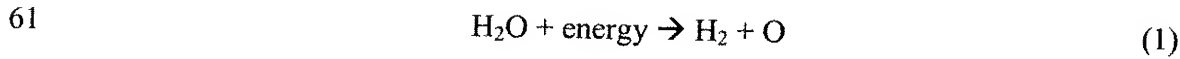
50

51 A good review of the field can be found in Johnson et al. (2003). Here we shall present a
52 brief summary of the literature published since then and at the same time describe each
53 O₂ production model. The focus will be on the chemical steps involved rather than the
54 kinetics of each model. Details of our experiments will then be given.

55

56 The papers by Johnson et al. (2003), Orlando and Sieger (2003) and Sieger et al. (1998)
57 culminated in the publication of Johnson et al. (2006) with what shall be referred to here
58 as the J(2006) model. This model proposes that O₂ is produced from the decomposition
59 of H₂O to H₂ and O-atoms.

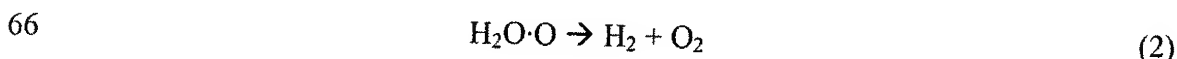
60



62

63 The O-atoms are trapped in the form of a stable precursor, possibly an H₂O·O complex,
64 before a second excitation produces H₂ and O₂.

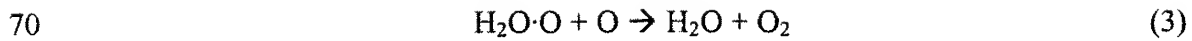
65



67

68 Alternatively a non-thermal O-atom from a secondary dissociation may form O₂.

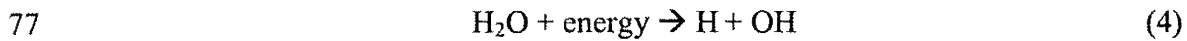
69



71

72 An alternative model recently proposed by Petrik et al. (2006), and which shall be
73 referred to here as the P(2006) model, proposes that the stable precursor is HO_2 and that
74 more steps are required than in the J(2006) model. First, H_2O is dissociated into H and
75 OH.

76

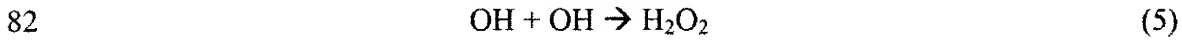


78

79 Next the OH, which is formed within the sample, migrates to the surface of the ice.

80 Multiple OH's then react to form H_2O_2 and subsequently HO_2 .

81



84

85 The hydroperoxy radical (HO_2) is then dissociated by an energetic excitation to form O_2 .

86



88

89 Both models predict very specific but different atomic and/or molecular intermediates,
90 yet in the experiments from which these models are constructed, the researchers never
91 actually identified any of the chemical intermediates.

92

93 The direct detection of radiolytically produced O-atom in an ice sample poses many
94 experimental challenges. Perhaps the best evidence for the production of O-atoms in ice
95 in the literature is found in the work of Matich et al. (1993) that detected Herzberg
96 emission lines of O₂ in UV-irradiated water ice. The authors reasoned that the O₂ was
97 formed from O-atom recombination, although other reactions not involving O-atoms
98 were possible. Here we present new laboratory results on the observation of O-atom
99 production in H₂O ice using the detection of isotopologues of ozone in irradiated H₂O +
100 ¹⁸O₂ thin-film samples.

101

102 The experimental details are similar to those described in Cooper et al. (2006). In brief,
103 we prepared gaseous mixtures of H₂¹⁶O + ¹⁸O₂ (6:1) in a vacuum manifold. Millipore
104 water was freeze-pump-thaw cycled multiple times to remove dissolved atmospheric
105 gases. The ¹⁸O₂ (Isotec; purity of > 97%) was used without further purification. Blank
106 experiments on irradiated pure ¹⁸O₂ produced ¹⁸O₃ and no other detectable scrambled
107 isotopes. The H₂O + ¹⁸O₂ gaseous mixtures were then deposited onto an aluminum
108 mirror, pre-cooled to 10 K by a closed-cycle helium refrigerator. The samples were then
109 warmed to 80 K, at ~2 K/min. The 80 K irradiation temperature was chosen to
110 approximate ice temperatures on the Galilean satellites. An increase in the vacuum-
111 chamber's base pressure when the pre-irradiated ice was warmed to ~30 K indicated that
112 some of the O₂ sublimed out of the sample. This observation is consistent with previous
113 work (Loeffler et al. 2006). Due to the sublimation of some of the O₂, the exact H₂O/O₂
114 ratio in the irradiated ice is unknown. The samples were then irradiated at 80 K with 0.8

115 MeV protons generated by a Van de Graaff accelerator. IR spectra were measured using a
116 Nicolet 6700 Nexus spectrometer at 4 cm⁻¹ spectral resolution.

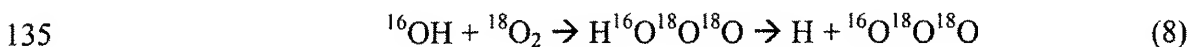
117

118 Figure 1 shows spectra of a H₂¹⁶O + ¹⁸O₂ sample before and after irradiation. As the dose
119 increased two broad but shallow absorption bands appeared at 980 and 990 cm⁻¹
120 associated with the formation of the 888 and 886 isotopologues, where 8 represents an
121 ¹⁸O-atom and 6 represents a ¹⁶O-atom. The 888 was produced from residually trapped
122 ¹⁸O₂ molecules that were nearest neighbors. The irradiation of pure ¹⁸O₂ did not yield any
123 measurable ozone isotopes containing ¹⁶O and there was no measurable amount of CO₂
124 atmospheric contaminant in our sample, so the ¹⁶O-atom in the 886 must have been
125 produced from H₂O. This was the first ozone mixed isotopologue observed as the dose
126 increased, and it is thought to be due to the first reaction step shown in Figure 2, i.e. the
127 combination of a radiolytically produced ¹⁶O-atom from water with ¹⁸O₂ that was trapped
128 in the ice. The 888 species was gradually destroyed (as shown in Figure 2) with
129 increasing dose by the replacement of ¹⁸O by radiolytically-produced ¹⁶O to form 886.

130

131 We considered the possibility that the source of ¹⁶O in these experiments could be ¹⁶OH
132 formed in the radiolytic destruction of H₂O. An ozone molecule containing a ¹⁶O-atom
133 could then be produced by the following reactions.

134



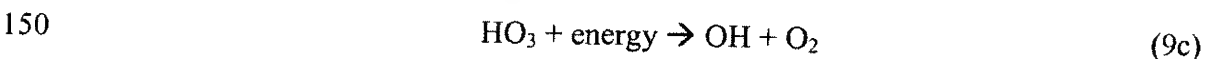
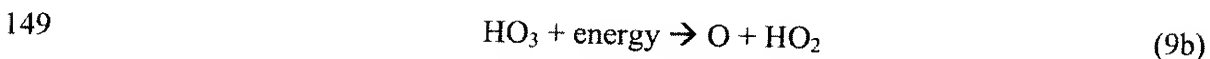
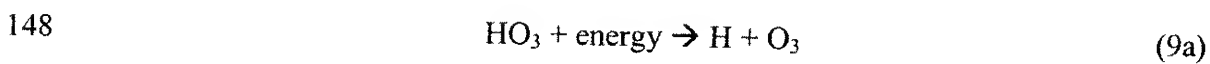
136

137 However, calculations by Varandas (2002) and Yu and Varandas (2001) show that
138 reaction 8 probably does not occur to any great extent since the energy of the HO₃
139 intermediate is only marginally below that of OH + O₂ on the ground-state HO₃ potential
140 energy surface. These workers have shown that the O + HO₂ and H + O₃ states are
141 accessible in the gas-phase when the reacting O₂ and OH are in highly excited vibrational
142 states. These excited states are likely to be very rapidly quenched in the cold ices
143 discussed in the present work.

144

145 Radiolytic dissociation from a stable HO₃ precursor (Reactions 9a-c) could also be
146 possible.

147



151

152

153 However, from the potential energy surface (Varandas, 2002), reaction 9c would be
154 expected to dominate due to the small difference in potential energy. Reaction 9a would
155 be the least significant due to the largest difference in potential energy of reactants and
156 products. In addition, the HO₃ abundance in irradiated H₂O + O₂ ices at 80 K is small
157 compared with the amount at 10 K (Cooper et al. 2006).

158

159

160 Once the 886 ozone species is produced, further reactions can occur. Other radiolytic
161 ^{16}O -atoms may add to either end of the 886 molecule and displace an O-atom from the
162 opposite end. Alternatively, an ozone isotopologue may decompose to a molecular
163 oxygen isotopologue and an O-atom (16 or 18). A ^{16}O -atom originating from radiolyzed
164 water may then react with the O_2 isotopologue to form either the 686 or 866 species
165 which are observed at 1003 and 1022 cm^{-1} respectively. The 866 can then form 686 or
166 666, and the 686 may form 866 which can feedback into the former reaction channel. The
167 666 isotopologue is observed at 1035 cm^{-1} . The positions of these isotopologues are
168 summarized in Table 1.

169

170 Assuming that oxygen atoms cannot add in between two other O-atoms in an ozone
171 molecule, the 868 isotopologue would need to form from the reaction between an 886 or
172 686 molecule and an ^{18}O -atom. The absence of the 868 ($\sim 1016\text{ cm}^{-1}$) isotopologue in the
173 sample indicates that ^{18}O is irreversibly lost to the water lattice once it is displaced. This
174 suggests that the amount of ^{16}O produced radiolytically from H_2O , must dominate the
175 amount of ^{18}O in the sample.

176

177 In our experiments on pure H_2O , we see no infrared evidence of ^{16}O -atom production via
178 the formation of molecular oxygen because the oxygen absorption band is very weak.
179 Ozone is also not produced in any detectable quantity because the amount of O_2 , the
180 precursor needed for O_3 production, is too small. However, when $^{18}\text{O}_2$ is added to pure
181 water, as described above, it acts as a trap for ^{16}O -atoms via the formation of ozone
182 isotopologues that can be detected spectroscopically.

183

184 Using a band strength of 1.4×10^{17} cm molecule⁻¹ (Smith et al. 1985) for the ν_3 feature of
185 O₃, and assuming that it is the same for all isotopologues, we have calculated that there
186 are 0.14% ¹⁶O-atoms by number relative to H₂O (Table 2) at the highest dose of 9.8
187 eV/16-amu molecule. In pure water ice, without the presence of ¹⁸O₂ to trap ¹⁶O-atoms as
188 an ozone isotopologue, it could be argued that the highly reactive ¹⁶O-atom may react
189 with water or another water radiation fragment (such as H or OH) before ever
190 encountering a second radiolytically produced ¹⁶O-atom. The lifetime of a single ¹⁶O-
191 atom surrounded by H₂O in an ice lattice is unknown, but it may be stabilized via
192 forming a complex with H₂O (Khriachtchev et al., 2000). However, if the ozone
193 isotopologues produced in the present work were dissociated and the ¹⁶O-atoms were to
194 reform exclusively as ¹⁶O₂, then there would be 0.07% ¹⁶O₂ by number, relative to H₂O.
195 This small amount of O₂ in pure water is far below the detection limits of our
196 spectrometer, but using the O₃ tracer molecule we can detect ¹⁶O-atoms that could
197 otherwise form O₂.

198

199 We note that these abundance estimates are calculated at the highest radiation dose of 9.8
200 eV/16-amu molecule used in the present experiments. At this dose, ¹⁶O-atom production
201 does not appear to be at steady-state (Figure 3) i.e. the yield of O-atoms has not reached a
202 point where the O-atom abundance doesn't change with increasing dose. However,
203 determining whether the O-atom production is at steady-state is impossible in these
204 experiments because we cannot measure all of the O-atoms. We can only observe the O-
205 atoms that are present as an ozone isotopologue. Previous experiments from our

206 laboratory (Cooper et al, 2008) have shown that in $\text{H}_2\text{O} + {}^{16}\text{O}_2$ ices that O_3 production
207 reaches steady-state by ~ 5 eV/16-amu molecule.

208

209 It is common in radiation chemistry to present production rates as a yield, G , the number
210 of molecules produced per 100 eV of energy absorbed. We have calculated an effective
211 $G_{\text{H}+}({}^{16}\text{O})$ by plotting the number of ${}^{16}\text{O}$ -atoms measured in ozone isotopologues as a
212 function of radiation dose (Figure 3). The slope of Figure 3 is 0.013, a value equal to
213 $G_{\text{H}+}({}^{16}\text{O})$. Again however, this value represents a lower limit due to the O-atoms that
214 cannot be directly measured in this experiment and is only an effective G-value as we are
215 actually not measuring ${}^{16}\text{O}$ -atoms directly, but indirectly in the form of ozone
216 isotopologues.

217

218 Estimates of the O_2 abundance on Ganymede range from 0.1 - 1.0% (Calvin et al. 1996)
219 to 1.4 - 4.2% (Hand et al. 2006). While our percentage abundance is lower than these
220 estimates, our value represents a lower limit estimate that is in good agreement with the
221 planetary observations. In these laboratory experiments we cannot account for the ${}^{16}\text{O}$ -
222 atoms that remain trapped in the ice and do not react, or the ${}^{16}\text{O}_2$ that is formed but is
223 present at a level below our detection limits because of the extremely weak fundamental
224 vibration, and also the ${}^{16}\text{O}_2$ formed that is sputtered or desorbed out of the sample. In
225 addition, other trapping mechanisms such as clathrates (Hand et al. 2006) or simultaneous
226 irradiation and deposition (Teolis et al. 2006), may increase the amount of O_2 trapped in
227 an icy satellite.

228

229 In terms of modeling the radiation processes that produce O₂ in pure H₂O, we have found
230 that O-atoms produced in these experiments, support the J(2006) model. While it does
231 not by any means conclusively prove the model is correct, it does provide added support
232 via the observation that O-atoms can be produced directly from H₂O molecules. The
233 P(2006) model does not consider the production of such O-atoms in the formation of O₂.
234 Further research is needed to produce a robust and accurate model for the formation of O₂
235 in irradiated, pure water ice, but we have shown here that O-atoms, produced directly
236 from water may play a part. The actual mechanism will likely require a multi-instrument
237 approach to detect all the intermediate species and reactions. In addition, further
238 laboratory work needs to be performed to understand the trapping mechanism of O₂ on
239 icy satellites.

240

241 Nevertheless, we have shown that O-atoms are produced directly from H₂O molecules in
242 an H₂O ice. If these O-atoms recombine to form O₂ in similarly irradiated water ice, a
243 lower abundance limit of 0.07% by number relative to water could result. This value
244 agrees with the observed O₂ abundance on Ganymede (Calvin et al, 1996; Hand et al,
245 2006).

246

247 REFERENCES

248 Calvin, W. M., R. E., Johnson, and J. R., Spencer (1996), O₂ on Ganymede: Spectral
249 characteristics and plasma formation mechanisms. *Geophys. Res. Lett.*, 23, 673-676.

250 Cooper, P. D., M. H. Moore, and R. L. Hudson (2006), Infrared detection of HO₂ and
251 HO₃ radicals in water ice, *J. Phys. Chem.* 110, 7985-7988.

252 Cooper, P. D., M. H. Moore, and R. L. Hudson (2008), Radiation Chemistry of H₂O + O₂
253 ices, *Icarus*, 194, 379-388.

254 Hand, K. P., C. F. Chyba, R. W. Carlson, J. F. Cooper (2006), Clathrate hydrates of
255 oxidants in the ice shell of Europa, *Astrobiol.* 6, 463-482.

256 Johnson, R. E., T. I. Quickenden, P. D. Cooper, A. J. McKinley, and C. G. Freeman
257 (2003), The production of oxidants in Europa's surface, *Astrobiol.* 3, 823-850.

258 Johnson, R. E., P. D. Cooper, T. I. Quickenden, G. A. Grieves, and T. M. Orlando,
259 (2005), Production of oxygen by electronically induced dissociations in ice, *J. Chem.*
260 *Phys.* 123, 184715.

261 Johnson, R. E., et al. (2006), Production, ionization and redistribution of O₂ in Saturn's
262 ring atmosphere, *Icarus*, 180, 393-402.

263 Khriachtchev, L., M. Pettersson, S. Jolkkonen, S. Pehkonen, and M. Rasanen (2000),
264 Photochemistry of hydrogen peroxide in Kr and Xe matrixes, *J. Chem. Phys.* 112,
265 2187-2194.

266 Loeffler, M. J., B. D., Teolis, and R. A. Baragiola (2006). A model study of the thermal
267 evolution of astrophysical ices, *Astrophys. J.* 639, L103-106.

268 Orlando, T. M., and M. T. Sieger (2003), The role of electron-stimulated production of
269 O₂ from water ice in the radiation processing of outer solar system surfaces, *Surf. Sci.*,
270 528, 1-7.

271 Petrik, N. G., A. G. Kavetsky, and G. A. Kimmel (2006), Electron-stimulated production
272 of molecular oxygen in amorphous solid water, *J. Phys. Chem. B.* 110, 2723-2731.

273 Schriver-Mazzuoli, L., A. Schriver, C. Lugez, A. Perrin, C. Camy-Peyret, and J.-M.
274 Flaud (1996) Vibrational spectra of the $^{16}\text{O}/^{17}\text{O}/^{18}\text{O}$ substituted ozone molecule
275 isolated in matrices, *J. Mol. Spec.*, 176, 85-94.

276 Sieger, M. T., W. C. Simpson, and T. M. Orlando (1998), Production of O_2 on icy
277 satellites by electronic excitation of low-temperature water ice. *Nature*, 394, 554-556.

278 Smith, M.A.H., C.P., Rinsland, B., Fridovich, and K. N. Rao, (1985), *Molecular*
279 *Spectroscopy: Modern Research, Volume 3*. Academic Press, London, UK.

280 Spencer, J. R., W. M. Calvin, and M. J. Person (1995), Charged-coupled device spectra
281 of the Galilean satellites: Molecular oxygen on Ganymede, *J. Geophys. Res.*, 100,
282 19049.

283 Spencer, J. R., and W. M. Calvin (2002), Condensed O_2 on Europa and Callisto, *Astron.*
284 *J.*, 124, 3400-3403.

285 Teolis, B. D., M. J. Loeffler, U. Raut, M. Fama, and R. A. Baragiola (2006), Ozone
286 synthesis on the icy satellites, *Astrophys. J.*, 644, L141-L144.

287 Tokar R.L., et al. (2005), Cassini observations of the thermal plasma in the vicinity of
288 Saturn's main rings and the F and G rings, *Geophys. Res. Lett.*, 32 (14): Art. No.
289 L14S04.

290 Varandas A. J. C. (2002), On the "ozone deficit problem": What are O_x and HO_x catalytic
291 cycles for ozone depletion hiding? *Chem. Phys. Chem.*, 3, 433-441.

292 Yu, H. G., and A. J. C. Varandas (2001), Ab initio theoretical calculation and potential
293 energy surface for ground-state HO_3 , *Chem. Phys. Lett.*, 334, 173-178.

294

295 **Table 1:** IR band positions (cm⁻¹) for the ν_3 vibration of ozone isotopologues in the gas-
 296 phase (Schriger et al. 1996) and in the present work in water ice.

	¹⁸ O ¹⁸ O ¹⁸ O	¹⁸ O ¹⁸ O ¹⁶ O	¹⁶ O ¹⁸ O ¹⁶ O	¹⁸ O ¹⁶ O ¹⁸ O	¹⁸ O ¹⁶ O ¹⁶ O	¹⁶ O ¹⁶ O ¹⁶ O
Gas-phase ^a	984.8	993.9	1008.5	1019.4	1028.1	1042.1
In ice (this work)	980	990	1003	-	1022	1035

297

298

299

300

301 **Table 2.** Percentage abundance of ozone isotopologues and the equivalent percentage
 302 abundance of ¹⁶O-atoms in irradiated H₂¹⁶O + ¹⁸O₂ ice at 80 K after a dose of 9.8 eV/16-
 303 amu molecule.

304

	Ozone Isotopologues			
	666	668	686	886
% abundance	0.024%	0.024%	0.006%	0.009%
% abundance of ¹⁶O-atoms	0.072%	0.048%	0.012%	0.009%
Total % abundance of ¹⁶O-atoms	0.14%			

305

306

307

308 **Figure 1:** The absorption bands of ozone isotopologues produced in an $\text{H}_2^{16}\text{O} + ^{18}\text{O}_2$ ice
309 sample irradiated with 0.8 MeV protons.

310

311 **Figure 2:** The chemical pathway for the formation of each ozone isotopologue. This
312 model assumes that ^{16}O only reacts with one end of an O_3 isotopologue and results in the
313 loss of an O-atom from the opposite end.

314

315 **Figure 3:** The dose dependent ^{16}O -atom production (measured as an ozone isotopologue)
316 at 80 K in an $\text{H}_2\text{O} + ^{18}\text{O}_2$ ice sample irradiated with 0.8 MeV protons.

317

318

319

320

321

322

323

324

325

326

327

328

329

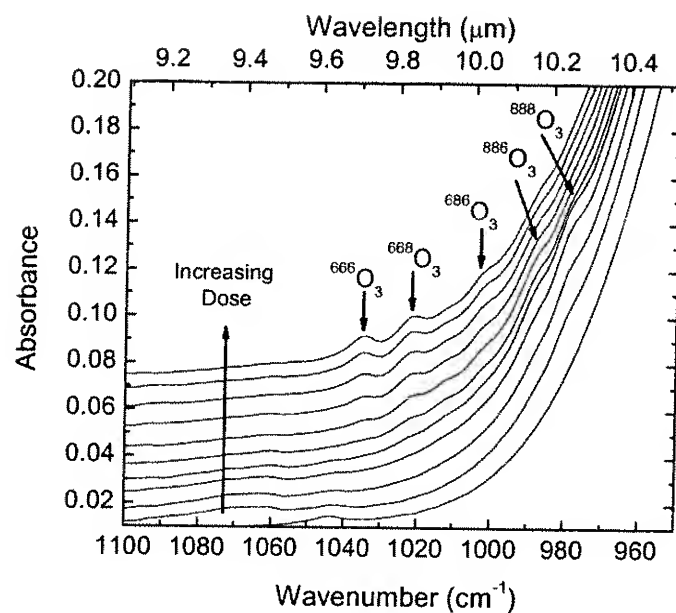
330

331

Figure 1

332

333



334

335

336

337

338

339

340

341

342

343

344

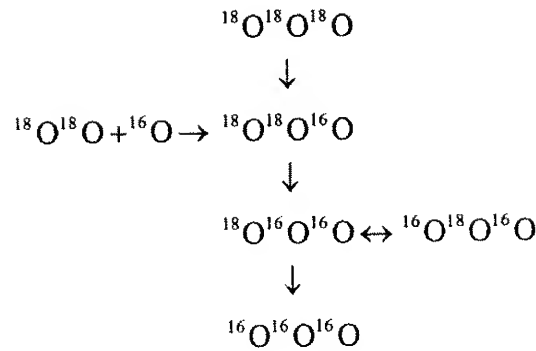
345

346

Figure 2

347

348



349

350

351

352

353

354

355

356

357

358

359

360

361

362

363

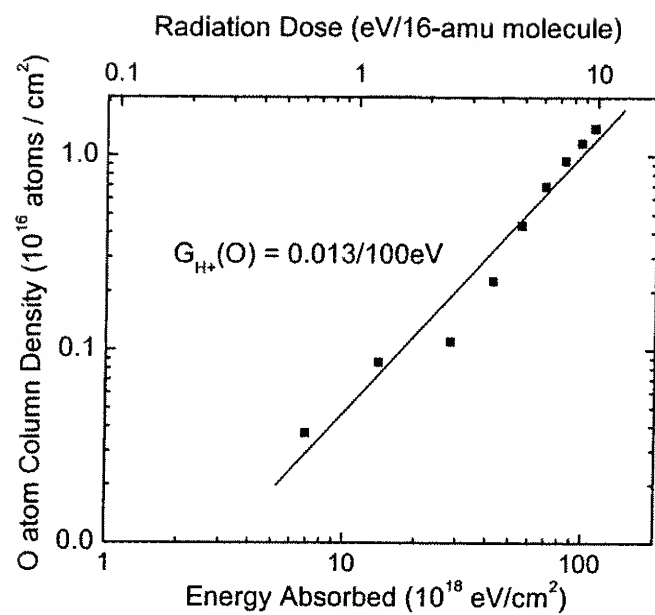
364

365

366

Figure 3

367



368